

Accepted Manuscript

Tricyclic pyrazolo[1,5-*d*][1,4]benzoxazepin-5(6H)-one scaffold derivatives: Synthesis and biological evaluation as selective BuChE inhibitors

Shi-Chao Chen, Guo-Liang Qiu, Bo Li, Jing-Bo Shi, Xin-Hua Liu, Wen-Jian Tang



PII: S0223-5234(18)30124-7

DOI: [10.1016/j.ejmech.2018.02.002](https://doi.org/10.1016/j.ejmech.2018.02.002)

Reference: EJMECH 10179

To appear in: *European Journal of Medicinal Chemistry*

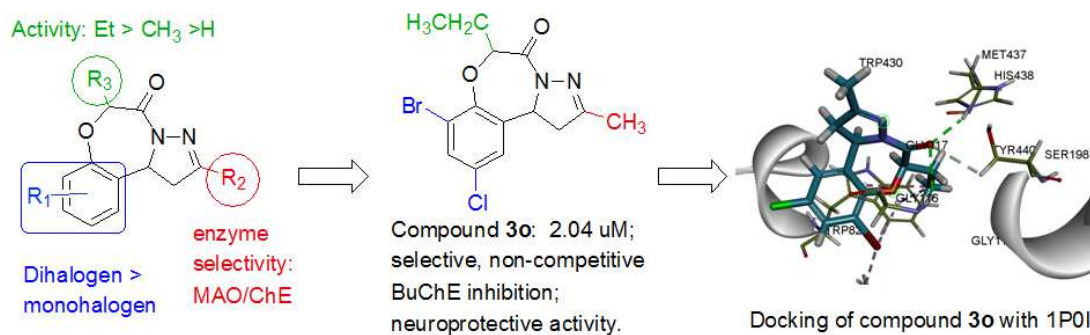
Received Date: 5 October 2017

Revised Date: 30 January 2018

Accepted Date: 2 February 2018

Please cite this article as: S.-C. Chen, G.-L. Qiu, B. Li, J.-B. Shi, X.-H. Liu, W.-J. Tang, Tricyclic pyrazolo[1,5-*d*][1,4]benzoxazepin-5(6H)-one scaffold derivatives: Synthesis and biological evaluation as selective BuChE inhibitors, *European Journal of Medicinal Chemistry* (2018), doi: 10.1016/j.ejmech.2018.02.002.

This is a PDF file of an unedited manuscript that has been accepted for publication. As a service to our customers we are providing this early version of the manuscript. The manuscript will undergo copyediting, typesetting, and review of the resulting proof before it is published in its final form. Please note that during the production process errors may be discovered which could affect the content, and all legal disclaimers that apply to the journal pertain.



Novel tricyclic scaffolds were discovered as selective BuChE inhibitors. Compounds **3f** and **3o** with dihalogen and a 6-ethyl substituent exhibited the most potent activity. Compound **3o** showed remarkable neuroprotective activity.

Tricyclic pyrazolo[1,5-*d*][1,4]benzoxazepin-5(6H)-one scaffold derivatives: Synthesis and biological evaluation as selective BuChE inhibitors

Shi-Chao Chen¹, Guo-Liang Qiu¹, Bo Li, Jing-Bo Shi, Xin-Hua Liu^{*}, Wen-Jian Tang^{*}

School of Pharmacy, Anhui Province Key Laboratory of Major Autoimmune Diseases, Anhui Institute of Innovative Drugs, Anhui Medical University, Hefei 230032, China.

Abstract: BuChE inhibitors play important roles in treatment of patients with advanced Alzheimer's disease (AD). A series of tricyclic pyrazolo[1,5-*d*][1,4]benzoxazepin-5(6H)-one derivatives were synthesized and evaluated as acetylcholinesterase (AChE) and butyrylcholinesterase (BuChE) inhibitors. Some derivatives showed selective BuChE inhibitory activity, which was influenced by the volumes of the substituted groups at the C6 position and halogen substituents at the benzene ring of tricyclic scaffold. Among them, compounds **3f** and **3o** with dihalogen and 6-ethyl substituent showed the most potent activity ($IC_{50} = 2.95, 2.04 \mu M$, and mixed-type, non-competitive inhibition against BuChE, respectively). Eutomer (**6R**)-**3o** exhibited better BuChE inhibitory activity than (**6S**)-**3o**. Compound **3o** exhibited nontoxic, good ADMET properties, and remarkable neuroprotective activity. Docking studies revealed the same binding orientation within the active site of target enzyme. Compound **3o** was nicely bound to BuChE *via* three hydrogen bonds, one Alkyl interaction and three Pi-Alkyl interactions. The selective BuChE inhibitors had a potential use in progressive neurodegenerative disorder.

Keywords: tricyclic; pyrazolo[1,5-*d*][1,4]benzoxazepin-5(6H)-one; acetylcholinesterase; butyrylcholinesterase; Alzheimer's disease; kinetic study

*Corresponding author.

Tel. & fax: +86 551 65161115. E-mail: xhliuhx@163.com; ahmupharm@126.com.

¹ S.C. Chen and G.L. Qiu contributed equally to this work.

1. Introduction

Alzheimer's disease (AD) is a chronic neurodegenerative disease that is characterized by progressive deterioration of memory and other cognitive functions [1]. As summarized in World Alzheimer Report 2016, 47 million people are living with dementia worldwide, and this number is estimated to increase to more than 131 million by 2050 [2]. β -Amyloid oligomerization [3], tau-protein hyperphosphorylation [4], cholinergic dysfunction [5], and oxidative stress [6], etc. are all responsible for pathogenesis of AD [7]. As the most effective therapeutic strategies, cholinergic dysfunction hypothesis directly contributes to cognitive decline [8]. It has been found that amyloid protein plaques can be caused by both cholinesterases (ChEs), named as acetylcholinesterase (AChE) and butyrylcholinesterase (BuChE), their inhibitors can decrease those plaques [9]. Moreover, abnormalities in cholinergic system are also closely related to other neurodegenerative disorders, such as PD, dementia with Lewy bodies and vascular dementia [10,11].

Therefore, administration of ChE inhibitors is a useful approach to elevate ACh levels within the brain [12,13]. ACh could be hydrolyzed by both AChE and BuChE, but BuChE is less substrate specific than AChE [14]. ACh levels increased 16-fold in wild-type mice treated with a selective AChE inhibitor, while no increase with a selective BuChE inhibitor [15]. AChE plays the major role in the hydrolysis of ACh in the healthy brain, while BuChE takes over the hydrolysis of ACh in the AChE deficient brain [16,17]. In AChE deficient mice, levels of excessive hippocampal ACh were alleviated by BuChE activity [18]. To avoid the adverse effects caused by suppression of AChE, development of effective and selective BuChE inhibitors to elevate ACh level in progressed AD is potentially advantageous [19,20]. Although the absence of BuChE has no significant adverse effects on health individuals, the recent finding that BuChE-catalyzed ghrelin hydrolysis influences mouse aggression and social stress may have potential implications for humans [21]. Marketed AD drugs except for memantine are all ChEs inhibitors, but donepezil and galantamine are selective AChE inhibitors, only rivastigmine is a dual AChE-BuChE inhibitor.

BuChE is a potential therapeutic target for restoring ACh levels in the brain, improving

cognitive impairment, reducing adverse effects in progressed AD patients. Although there are different types of scaffolds with BuChE inhibition, scaffolds of selective BuChE inhibitors are far from abundance [22,23]. As the multifactorial neurodegenerative disease, another trend of AD therapy is focused on multiple targeted ligands, where mostly ChE inhibition is combined with additional biological properties, along affecting monoamine oxidases (MAOs) metabolism as well as mitochondrial functions, and antioxidant properties [24–29]. Moreover, inhibition of enzymatic activities of MAOs and ChEs has been pursued to identifying novel therapeutic agents with a potential disease-modifying effect [30–32]. Thus, it is expected to discover more and more potential ChE inhibitors with diverse structures.

In our recent work, a novel tricyclic scaffold of pyrazolo[1,5-*d*][1,4]benzoxazepin-5(6H)-one was found to be a selective hMAO-B inhibitor [33,34], which are used alone or in combination to treat Alzheimer's and Parkinson's diseases [35,36]. Based on multi-target property of AD therapy, ChEs inhibitory activities of this tricyclic scaffold were screened to discover novel ChE inhibitors, but they showed weak inhibitory activities for AChE and BuChE. When 2-aryl group of the tricyclic scaffold was substituted by methyl group, new tricyclic compounds exhibited moderate inhibitory activities against ChE and weak inhibitory activities against MAOs. It implied that 2-substituent of tricyclic scaffold may lead to the change of enzymatic inhibitory activities between MAOs and ChEs (Fig. 1). Herein, based on above rational analysis, a series of pyrazolo[1,5-*d*][1,4]benzoxazepin-5(6H)-one derivatives were designed and synthesized as selective cholinesterase inhibitors. Further, the most potent compounds will be used to study the preliminary mechanism.

(Fig. 1)

2. Results and discussion

2.1. Chemistry

According to our recent works [33,34], pyrazolo[1,5-*d*][1,4]benzoxazepin-5(6H)-one derivatives (**3a–3s**, as shown in Table 1) were synthesized according to the protocol

outlined in Scheme 1. The key intermediate 2-pyrazoline (**1**) was obtained by the cyclization reaction of excess hydrazine hydrate with the styrene ketones, which were prepared through Claisen-Schmidt condensation of substituted salicylaldehyde with acetone. The acylation of compound **1** with α -bromoacyl chloride gave 2-pyrazoline-1-ethanone derivatives (**2**). The title compounds **3a–3s** were obtained through the cyclization reaction of compound **2** in the presence of NaHCO_3 catalysis in ethanol. The total yield was 14% – 23%. Compounds **3t–3x** were synthesized according to the literature procedure [34].

To further study a possible influence of chirality at C-6 on ChE inhibitory activity, two enantiomers of compound **3o** were synthesized by the acylation of 2-bromo-4-chloro-6-(3-methyl-4,5-dihydro-1H-pyrazol-5-yl)phenol with chiral pure 2-chloropropionic acid and subsequent cyclization reaction in 32% and 34% yield respectively (Scheme 2).

(Scheme 1)

(Scheme 2)

2.2. Inhibitory activity against AChE and BuChE

The inhibitory potency of compounds **3a–3x** was assessed by Ellman's assay on *Electrophorus electricus* AChE (EeAChE) and equine BuChE (eqBuChE) [37]. The IC_{50} values were obtained and compared to the reference donepezil, a selective AChE inhibitor, which was the only one of four FDA-approved AChEIs that simultaneously binds to catalytic active and peripheral anionic sites, providing moderate inhibition of A β aggregation [38,39]. The IC_{50} values of all tested compounds against EeAChE and eqBuChE were summarized in Table 1.

(Table 1)

Enzymatic assays revealed that 26 tricyclic compounds exhibited inhibitory activities against cholinesterases, among them, some compounds showed potent BuChE inhibition. It was obvious from the data that compounds **3f** and **3o** exhibited the best activities

against BuChE with IC_{50} values of 2.95 and 2.04 μM , respectively, surpassing that of the positive control donepezil ($IC_{50} = 11.81 \mu\text{M}$). Inspection of the chemical structures, it can be concluded that the BuChE inhibitory activity was related to the substituent groups at C2, C6, C8 and C10 positions of benzoxazepinone moiety (Table 1). From Table 1, it is intuitive that the volume of the substituted group at the C2 position of the pyrazole ring plays an important role in the activity. The methyl group at the C2 position can increase the inhibitory activity against BuChE. For example, compound **3b** has an IC_{50} value of 5.95 μM against BuChE; when the C2 position is furan (compound **3u**), the inhibition rate is 23% at 20 μM .

Compounds with halogen substituents at the benzene ring in the benzoxazepinone moiety have great influence on the BuChE inhibition, for example, compounds **3a–3o** with 8- or/and 10-halogen substitutions at the benzene ring were found better in terms of potency than the corresponding compounds **3p–3s** with methyl or methoxyl substituents. Compound **3o** with 8-bromo and 10-chloro substituents showed more potent BuChE inhibitory activity ($IC_{50} = 2.04 \mu\text{M}$) than the non-halogen substituted compounds **3p–3s** (inhibition rate at 20 $\mu\text{M} < 5\%$).

From Table 1, it is observed that the volumes of the substituted groups at the C6 position of the seven-membered ring have significant influences on the BuChE activity. Along with the big substituent, the inhibitory activity was increased significantly. When the substituents at the R_2 position are H, methyl and ethyl respectively, the BuChE inhibitory activity were increased gradually. For example, compound **3a** has an inhibition 31% at 20 μM against BuChE; when the R_2 position is methyl (compound **3b**), the IC_{50} value was changed to 5.95 μM ; when the R_2 position is ethyl (compound **3c**), the IC_{50} value was changed to 4.67 μM . This trend can also be observed among others compounds (**3g, 3h, 3i, 3j, 3k, 3l, 3m, 3n, 3o** except for **3e < 3d < 3f**).

To observe the influence of chiral C-6 on ChE inhibitory activity, enantiomers (**6R**)-**3o** and (**6S**)-**3o** were synthesized. Regarding BuChE affinity, an eudismic ratio equal to 18 was observed for both racemates. Eutomer (**6R**)-**3o** exhibited much better BuChE inhibitory activity than isomer (**6S**)-**3o** ($IC_{50} = 1.14$ and 20.42 μM , respectively).

2.3 Kinetic Study of eqBuChE inhibition

The kinetic studies for the most active compounds **3f** and **3o** were carried out at three fixed inhibitor concentrations (5 μM , 10 μM and 20 μM). In each case, the kinetic type of enzyme inhibition was obtained through the modified Ellman's method and Lineweaver–Burk secondary plots [40]. As shown in Fig. 2A, overlaid reciprocal Lineweaver–Burk plots showed both higher slopes (decreased V_{max}) and intercepts (higher K_m) at increasing inhibitor concentrations, a trend that is generally ascribed to a mixed-type inhibition. In the same way, Fig. 2B showed all lines intersect the x-axis, it confirmed the typical characteristics of non-competitive inhibitors. The dissociation constants K_i for compounds **3f** (Fig. 2C) and **3o** (Fig. 2D) were estimated to be 7.60 μM and 1.50 μM , respectively.

(Fig. 2.)

2.4 Cytotoxicity assays and Neuroprotective effect against H_2O_2 -induced cell death in PC12 neurons

The differentiated PC12 cells and H_2O_2 were selected as *in vitro* model and oxidative agent to assess neuronal differentiation and other neurobiochemical and neurobiological studies [41,42]. The neuroprotective activity of compound **3o** and donepezil against oxidative stress-induced cell death in differentiated PC12 neurons was evaluated. Thus, differentiated PC12 cells were pretreated with different concentrations (10, 25 and 50 μM) for 3 h, before treatment with H_2O_2 (300 μM), and cell viability was measured after 24 h by using the MTT assay. As shown in Fig. 3, compound **3o** (3A) and donepezil (3B) at the test concentrations (1–50 μM) had no obviously cytotoxicity in PC-12 cells, and the relative cell viabilities of treated cells were all more than 90%. Neuroprotective activity of the most potent compound **3o** against eqBuChE was assessed by subjecting PC12 cells to H_2O_2 -induced damage. As shown in Fig. 4, the percent of cell viability was calculated in comparison to control group. Compound **3o** exhibited remarkable neuroprotective activity at 25 μM (cell viability = 70%, and $p < 0.05$ vs H_2O_2 treatment alone).

(Fig. 3.)

(Fig. 4.)

2.5. Oil/water partition coefficient assessment and ADMET prediction

To evaluate the drug-like properties of active compounds, Lipinski's rule of five were used to predict the ADME profiles for active compounds, i.e., log P (o/w) (octanol-water partition coefficient), number of hydrogen bond donor atom, number of hydrogen bond acceptor atom, et al. As an important parameter to predict the ability to cross blood-brain barrier (BBB), the log P with the optimum central nervous system penetration was around 2.0 ± 0.7 [43,44]. The log P values of compounds **3b**, **3c**, **3f**, **3i**, **3l**, **3n** and **3o** were 2.49, 1.12, 1.08, 1.05, 1.11, 2.18 and 1.57, respectively (Table 2), which suggested that the active compounds are lipophilicity ($\log P < 5$).

The ADMET properties were considered critical parameters for drug candidates [45]. The active compounds were analyzed with the ADMET prediction tools of DS 2017R2. As shown in Table 3 and Fig. 5, they showed good absorption, good solubility, and medium to high penetrant. Predicted ADMET properties of active compounds are in an agreement with the log P values. These results indicated that compounds **3n** and **3o** were possible sufficiently lipophilic to pass the BBB *in vivo*.

(Table 2)

(Table 3)

2.6. Molecular docking

In order to gain more understanding of the structure–activity relationships for the BuChE, based on the X-ray crystal structure of human BuChE (*h*BuChE PDB ID: 1P0I), molecular docking was performed on the binding model using the Discovery Studio 2017R2 software [46,47]. The docking calculation of compounds **3a–3o**, **(6R)-3o** and **(6S)-3o** was depicted in Table 4, the results showed that compounds **3a–3o**, **(6R)-3o** and **(6S)-3o** had nice binding affinity to BuChE and their

CDOCKER_INTERACTION_ENERGY had the same trend as the BuChE inhibitory activities, which further proved the correlation between the BuChE inhibitory activity and binding energy.

(Table 4)

Among them, compound **30** showed the maximum -CDOCKER_INTERACTION_ENERGY, which suggested that it was mostly easy to bind to BuChE. The 2D and 3D binding models of compound **30** with BuChE were depicted in Fig. 6. The amino acid residues which had interactions with BuChE as well as bond lengths were labeled. In the binding models, compound **30** was nicely bound to BuChE *via* three hydrogen bonds with His438 (distance = 2.36 Å), Gly116 (distance = 3.04 Å) and Ser198 (distance = 2.85 Å). Specifically, two conventional hydrogen bond interactions arose between the C=O group at the C5 position of ligand **30** and the NH groups of His438 and Gly116. Moreover, carbon hydrogen bond interaction also arose between the C=O group of ligand **30** and the CH₂ group of Ser198. The above observations can explain the potent BuChE inhibition of compound **30**. In addition, compound **30** was also nicely bound to BuChE *via* one Alkyl interaction and three Pi-Alkyl interactions. The Alkyl interaction was formed between the end group of Leu125 and bromine, which increased inhibitory activities by strengthening the binding affinity. Three Pi-Alkyl interactions were formed between the end group of Trp82 and the methyl of the C6 position and 8-bromo substituent. Furthermore, the H-bonds surface of compound **30** and receptor BuChE was also depicted in Fig. 7. These docking results, along with the biological assay data, suggested that compound **30** possessed higher inhibitory activity than other compounds, which will help us carry out the next structure optimization.

(Fig. 6.)

(Fig. 7.)

3. Conclusions

In this work, we reported design and synthesis of a series of pyrazolo[1,5-*d*][1,4]benzoxazepin-5(6H)-one derivatives and evaluated *in vitro* AChE and BuChE activities. Some derivatives showed selective BuChE inhibitory activity. The SARs analysis showed that the volumes of the substituted groups at the C6 position and halogen substituent at the benzene ring have significant influences for the BuChE activity. Among them, compounds bearing dihalogen and 6-ethyl substituent showed the most potent activity ($IC_{50} = 2.95$ and $2.04 \mu\text{M}$, respectively). Eutomer (**6R**)-**3o** exhibited much better BuChE inhibitory activity than isomer (**6S**)-**3o** ($IC_{50} = 1.14$ and $20.42 \mu\text{M}$, respectively). Kinetic studies on substrate-enzyme relationship revealed that compounds **3f** and **3o** showed mixed-type and non-competitive inhibition against BuChE ($K_i = 7.60$ and $1.50 \mu\text{M}$, respectively). The active compounds were found to be nontoxic at their effective concentrations against BuChE and to have good ADMET property predictions. Compound **3o** demonstrated remarkable neuroprotective activity. Docking studies showed that these potent compounds had same binding orientation within the active site of target enzyme. Compound **3o** was nicely bound to BuChE *via* three hydrogen bonds with His438, Gly116 and Ser198, one Alkyl interaction and three Pi-Alkyl interactions. The active compounds are selective BuChE inhibitors with a potential use against progressive neurodegenerative disorder.

4. Experimental section

4.1. Chemistry

All reagents were purchased from commercial sources and were used without further purification. Melting points (uncorrected) were determined on a XT4MP apparatus (Taikhe Corp., Beijing, China). ^1H NMR and ^{13}C NMR spectra were recorded on Bruker AV-600 or

AV-300 MHz instruments in CDCl_3 . Chemical shifts are reported in parts per million (δ) downfield from the signal of tetramethylsilane (TMS) as internal standards. Coupling constants are reported in Hz. The multiplicity is defined by *s* (singlet), *d* (doublet), *t* (triplet), or *m* (multiplet). Optical rotations: WZZ-2S digital automatic polarimeter. High resolution mass spectra (HRMS) were obtained on an Agilent 1260-6221 TOF mass spectrometry. Column and thin-layer chromatography (CC and TLC, resp.) were performed on silica gel (200-300 mesh) and silica gel GF₂₅₄ (Qingdao Marine Chemical Factory) respectively.

4.1.1. General procedure for the preparation of compounds **3a–3s**

To a solution of salicylaldehyde (10 mmol) in acetone (20 mL) was added 40% NaOH aqueous solution (2 mL) dropwise and the reaction was stirred at 60 °C for 2 h. The mixture was poured into cold water and neutralized with 2 M HCl to a pH in the range of 5~6. The resulting precipitate was collected, washed with water and dried to give chalcones. The chalcone was treated with 5 times excess of hydrazine hydrate in ethanol and refluxed for 5 h. The reaction mixture was then poured into ice-cold water. The solid was filtered, washed and recrystallized from ethanol to afford respective pyrazoline (**1**). A solution of compound **1** in CH_2Cl_2 (20 mL) was added α -bromoacyl chloride (5.0 mmol) and 4-dimethylaminopyridine (6.0 mmol) and the reaction was stirred overnight. The reaction mixture was washed with water and brine, dried with anhydrous Na_2SO_4 , filtrated and concentrated *in vacuo*. The resulting residue was then purified by column chromatography to give product **2**. NaHCO_3 (3.0 mmol) was added to an ethanol (20 mL) solution of compound **2** (2.0 mmol), then the reaction mixture was stirred at 70 °C until the disappearance of starting material (monitored by TLC). EtOAc (100 mL) was added to the reaction mixture, then washed with water and brine, dried with anhydrous Na_2SO_4 , filtrated and concentrated *in vacuo*. The residue was purified by chromatography on a silica gel column (petroleum/EtOAc, 1:1 → 1:2) to give title compounds **3a–3s**.

4.1.1.1.

8,10-Dichloro-2-methyl-1,11b-dihydro-pyrazolo[1,5-d][1,4]benzoxazepin-5(6H)-one (3a). White powder, yield, 20%; m.p. 217–219°C; ^1H NMR (300 MHz, CDCl_3) δ 7.46 (d, *J* =

2.0 Hz, 1H), 7.14 (s, 1H), 5.83 (m, 1H, 11b-H), 5.01 (d, $J = 16.8$ Hz, 1H, 6-Hb), 4.43 (d, $J = 16.8$ Hz, 1H, 6-Ha), 3.42 (dd, $J = 17.9, 9.1$ Hz, 1H, 1-Hb), 3.27 (dd, $J = 17.9, 11.4$ Hz, 1H, 1H-a), 2.23 (s, 3H, 2-CH₃). TOF-HRMS: m/z [M + Na]⁺ calcd for C₁₂H₁₀Cl₂N₂NaO₂: 307.0012; found: 307.0014.

4.1.1.2.

8,10-Dichloro-2-methyl-6-methyl-1,11b-dihydro-pyrazolo[1,5-d][1,4]benzoxazepin-5(6H)-one (3b). White powder, yield, 18%; m.p. 228–230°C; ¹H NMR (600 MHz, CDCl₃) δ 7.43 (d, $J = 2.2$ Hz, 1H), 7.08 (d, $J = 1.8$ Hz, 1H), 5.69 (t, $J = 10.6$ Hz, 1H, 11b-H), 5.10 (q, $J = 6.9$ Hz, 1H, 6-Hb), 3.34 (dd, $J = 10.5, 4.6$ Hz, 2H, 1-H), 2.20 (s, 3H, 2-CH₃), 1.57 (s, 3H, 6-CH₃); ¹³C NMR (150 MHz, CDCl₃) δ 166.6, 157.8, 150.3, 132.6, 130.3, 129.4, 129.1, 124.8, 78.3 (C-6), 57.3 (11b-C), 42.0 (C-1), 17.3 (6-CH₃), 16.2 (2-CH₃). TOF-HRMS: m/z [M + Na]⁺ calcd for C₁₃H₁₂Cl₂N₂NaO₂: 321.0168; found: 321.0166.

4.1.1.3.

8,10-Dichloro-6-ethyl-2-methyl-1,11b-dihydro-pyrazolo[1,5-d][1,4]benzoxazepin-5(6H)-one (3c). White powder, yield, 17%; m.p. 219–221°C; ¹H NMR (300 MHz, CDCl₃) δ 7.37 (d, $J = 2.1$ Hz, 1H), 6.98 (d, $J = 1.6$ Hz, 1H), 5.71 (t, $J = 10.6$ Hz, 1H, 11b-H), 4.58 (t, $J = 6.5$ Hz, 1H, 6-Ha), 3.50 (dd, $J = 17.4, 11.1$ Hz, 1H, 1-Hb), 3.24 (dd, $J = 17.6, 10.0$ Hz, 1H, 1-Ha), 2.16 (s, 3H, 2-CH₃), 2.14 – 2.01 (m, 2H, 6-CH₂CH₃), 1.14 (t, $J = 7.4$ Hz, 3H, 6-CH₂CH₃). TOF-HRMS: m/z [M + Na]⁺ calcd for C₁₄H₁₄Cl₂N₂NaO₂: 335.0325; found: 335.0323.

4.1.1.4.

8,10-Dibromo-2-methyl-1,11b-dihydro-pyrazolo[1,5-d][1,4]benzoxazepin-5(6H)-one (3d). White powder, yield, 21%; m.p. 223–225°C; ¹H NMR (300 MHz, CDCl₃) δ 7.76 (d, $J = 1.9$ Hz, 1H), 7.31 (s, 1H), 5.83 (m, 1H, 11b-H), 5.00 (d, $J = 16.8$ Hz, 1H, 6-Hb), 4.44 (d, $J = 16.8$ Hz, 1H, 6-Ha), 3.42 (dd, $J = 18.0, 8.9$ Hz, 1H, 1-Hb), 3.27 (dd, $J = 18.0, 11.4$ Hz, 1H, 1-Ha), 2.23 (s, 3H, 2-CH₃); ¹³C NMR (75 MHz, CDCl₃) δ 163.5, 157.6, 153.9, 136.2, 134.8, 127.2, 118.5, 117.8, 71.5 (C-6), 55.8 (11b-C), 39.5 (C-1), 16.2 (2-CH₃). TOF-HRMS: m/z [M + Na]⁺ calcd for C₁₂H₁₀Br₂N₂NaO₂: 394.9001; found: 394.9002.

4.1.1.5.

8,10-Dibromo-2-methyl-6-methyl-1,11b-dihydro-pyrazolo[1,5-d][1,4]benzoxazepin-5(6H)-one (**3e**). White powder, yield, 18%; m.p. 243–245°C; ^1H NMR (300 MHz, CDCl_3) δ 7.72 (d, $J = 1.9$ Hz, 1H), 7.25 (d, $J = 1.1$ Hz, 1H), 5.68 (t, $J = 10.7$ Hz, 1H, 11b-H), 5.07 (q, $J = 6.9$ Hz, 1H, 6-Hb), 3.34 (d, $J = 10.6$ Hz, 2H, 1-H), 2.19 (s, 3H, 2- CH_3), 1.62 (s, 3H, 6- CH_3); ^{13}C NMR (75 MHz, CDCl_3) δ 166.5, 158.0, 152.0, 135.9, 132.2, 128.6, 118.4, 116.6, 78.0 (C-6), 57.4 (11b-C), 42.4 (C-1), 17.3 (6- CH_3), 16.2 (2- CH_3). TOF-HRMS: m/z $[\text{M} + \text{Na}]^+$ calcd for $\text{C}_{13}\text{H}_{12}\text{Br}_2\text{N}_2\text{NaO}_2$: 408.9158; found: 408.9160.

4.1.1.6.

8,10-Dibromo-6-ethyl-2-methyl-1,11b-dihydro-pyrazolo[1,5-d][1,4]benzoxazepin-5(6H)-one (**3f**). White powder, yield, 20%; m.p. 224–226°C; ^1H NMR (300 MHz, CDCl_3) δ 7.66 (d, $J = 1.7$ Hz, 1H), 7.14 (d, $J = 1.3$ Hz, 1H), 5.72 (t, $J = 10.6$ Hz, 1H, 11b-H), 4.56 (dd, $J = 7.6, 5.5$ Hz, 1H, 6-Ha), 3.52 (dd, $J = 17.6, 11.2$ Hz, 1H, 1-Hb), 3.23 (dd, $J = 17.7, 9.8$ Hz, 1H, 1-Ha), 2.15 (s, 3H, 2- CH_3), 2.09 (m, 2H, 6- CH_2CH_3), 1.15 (t, $J = 7.4$ Hz, 3H, 6- CH_2CH_3). TOF-HRMS: m/z $[\text{M} + \text{Na}]^+$ calcd for $\text{C}_{14}\text{H}_{14}\text{Br}_2\text{N}_2\text{NaO}_2$: 422.9314; found: 422.9311.

4.1.1.7. 10-Chloro-2-methyl-1,11b-dihydro-pyrazolo[1,5-d][1,4]benzoxazepin-5(6H)-one (**3g**). White powder, yield, 23%; m.p. 186–188°C; ^1H NMR (300 MHz, CDCl_3) δ 7.35 (dd, $J = 8.5, 2.3$ Hz, 1H), 7.21 (d, $J = 2.0$ Hz, 1H), 7.14 (d, $J = 8.5$ Hz, 1H), 5.85–5.73 (m, 1H, 11b-H), 4.96 (d, $J = 16.6$ Hz, 1H, 6-Hb), 4.39 (d, $J = 16.6$ Hz, 1H, 6-Ha), 3.44 (dd, $J = 17.9, 9.3$ Hz, 1H, 1-Hb), 3.26 (dd, $J = 17.9, 11.3$ Hz, 1H, 1-Ha), 2.23 (s, 3H, 2- CH_3); ^{13}C NMR (75 MHz, CDCl_3) δ 164.1, 157.9, 156.7, 132.7, 130.7, 130.6, 125.3, 123.1, 72.8 (C-6), 55.8 (11b-C), 39.7 (C-1), 16.2 (2- CH_3). TOF-HRMS: m/z $[\text{M} + \text{Na}]^+$ calcd for $\text{C}_{12}\text{H}_{11}\text{ClN}_2\text{NaO}_2$: 273.0401; found: 273.0394.

4.1.1.8.

10-Chloro-2-methyl-6-methyl-1,11b-dihydro-pyrazolo[1,5-d][1,4]benzoxazepin-5(6H)-one (**3h**). White powder, yield, 21%; m.p. 199–202°C; ^1H NMR (300 MHz, CDCl_3) δ 7.24

(d, $J = 2.3$ Hz, 1H), 7.13 (d, $J = 1.7$ Hz, 1H), 6.98 (d, $J = 8.6$ Hz, 1H), 5.74 (t, $J = 10.5$ Hz, 1H, 11b-H), 4.95 (q, $J = 6.8$ Hz, 1H, 6-Hb), 3.36 (d, $J = 11.4$ Hz, 2H, 1-H), 2.18 (s, 3H, 2-CH₃), 1.52 (d, $J = 6.8$ Hz, 3H, 6-CH₃); ¹³C NMR (75 MHz, CDCl₃) δ 166.8, 157.9, 154.1, 130.3, 129.5, 129.0, 126.4, 123.90, 76.3 (C-6), 57.5 (11b-C), 42.6 (C-1), 17.4 (6-CH₃), 16.2 (2-CH₃). TOF-HRMS: m/z [M + H]⁺ calcd for C₁₃H₁₄ClN₂O₂: 265.0738; found: 265.0739.

4.1.1.9.

10-Chloro-6-ethyl-2-methyl-1,11b-dihydro-pyrazolo[1,5-d][1,4]benzoxazepin-5(6H)-one (**3i**). White powder, yield, 19%; m.p. 188–190°C; ¹H NMR (300 MHz, CDCl₃) δ 7.23 (dd, $J = 8.7, 2.2$ Hz, 1H), 7.10 (s, 1H), 7.00 (d, $J = 8.6$ Hz, 1H), 5.74 (t, $J = 10.5$ Hz, 1H, 11b-H), 4.59 (dd, $J = 9.4, 4.0$ Hz, 1H, 6-Ha), 3.42 (dd, $J = 17.7, 11.1$ Hz, 1H, 1-Hb), 3.30 (dd, $J = 17.7, 9.9$ Hz, 1H, 1-Ha), 2.17 (s, 3H, 2-CH₃), 2.10 (ddd, $J = 14.7, 7.5, 4.1$ Hz, 1H, 6-CH₂CH₃), 1.92–1.72 (m, 1H, 6-CH₂CH₃), 1.11 (t, $J = 7.4$ Hz, 3H, 6-CH₂CH₃); ¹³C NMR (75 MHz, CDCl₃) δ 166.3, 157.9, 154.8, 129.4, 128.4, 126.8, 123.0, 101.5, 81.3 (C-6), 57.9 (11b-C), 43.5 (C-1), 24.0 (6-CH₂CH₃), 16.1 (2-CH₃), 10.4 (6-CH₂CH₃). TOF-HRMS: m/z [M + H]⁺ calcd for C₁₄H₁₆ClN₂O₂: 279.0895; found: 279.0896.

4.1.1.10.

10-Bromo-2-methyl-1,11b-dihydro-pyrazolo[1,5-d][1,4]benzoxazepin-5(6H)-one (**3j**). White powder, yield, 17%; m.p. 214–216°C; ¹H NMR (300 MHz, CDCl₃) δ 7.50 (dd, $J = 8.5, 1.8$ Hz, 1H), 7.36 (s, 1H), 7.08 (d, $J = 8.5$ Hz, 1H), 5.86 – 5.75 (m, 1H, 11b-H), 4.97 (d, $J = 16.6$ Hz, 1H, 6-Hb), 4.40 (d, $J = 16.6$ Hz, 1H, 6-Ha), 3.45 (dd, $J = 17.9, 9.4$ Hz, 1H, 1-Hb), 3.26 (dd, $J = 18.0, 11.3$ Hz, 1H, 1-Ha), 2.23 (s, 3H, 2-CH₃); ¹³C NMR (75 MHz, CDCl₃) δ 163.9, 157.7, 157.0, 133.4, 132.9, 128.0, 123.3, 118.0, 72.5 (C-6), 55.6 (11b-C), 39.5 (C-1), 16.1 (2-CH₃). TOF-HRMS: m/z [M + Na]⁺ calcd for C₁₂H₁₁BrN₂NaO₂: 316.9896; found: 316.9899.

4.1.1.11.

10-Bromo-2-methyl-6-methyl-1,11b-dihydro-pyrazolo[1,5-d][1,4]benzoxazepin-5(6H)-one (**3k**). White powder, yield, 18%; m.p. 218–220°C; ¹H NMR (300 MHz, CDCl₃) δ 7.39

(dd, $J = 8.5, 2.1$ Hz, 1H), 7.27 (s, 1H), 6.92 (d, $J = 8.6$ Hz, 1H), 5.74 (t, $J = 10.5$ Hz, 1H, 11b-H), 4.94 (q, $J = 6.8$ Hz, 1H, 6-Hb), 3.46–3.24 (m, 2H, 1-H), 2.18 (s, 3H, 2-CH₃), 1.52 (d, $J = 6.8$ Hz, 3H, 6-CH₃); ¹³C NMR (75 MHz, CDCl₃) δ 166.5, 157.8, 154.5, 132.3, 130.4, 129.2, 124.0, 116.1, 75.9 (C-6), 57.3 (11b-C), 42.6 (C-1), 17.2 (6-CH₃), 16.0 (2-CH₃). TOF-HRMS: m/z [M + H]⁺ calcd for C₁₃H₁₄BrN₂O₂: 309.0233; found: 309.0241.

4.1.1.12.

10-Bromo-6-ethyl-2-methyl-1,11b-dihydro-pyrazolo[1,5-d][1,4]benzoxazepin-5(6H)-one (3l). White powder, yield, 16%; m.p. 195–198°C; ¹H NMR (300 MHz, CDCl₃) δ 7.37 (dd, $J = 8.6, 2.2$ Hz, 1H), 7.24 (s, 1H), 6.94 (d, $J = 8.6$ Hz, 1H), 5.74 (t, $J = 10.5$ Hz, 1H, 11b-H), 4.58 (dd, $J = 9.4, 4.0$ Hz, 1H, 6-Ha), 3.43 (dd, $J = 17.6, 11.1$ Hz, 1H, 1-Hb), 3.30 (dd, $J = 17.6, 10.0$ Hz, 1H, 1-Ha), 2.17 (s, 3H, 2-CH₃), 2.14–2.01 (m, 1H, 6-CH₂CH₃), 1.91–1.76 (m, 1H, 6-CH₂CH₃), 1.11 (t, $J = 7.4$ Hz, 3H, 6-CH₂CH₃). TOF-HRMS: m/z [M + H]⁺ calcd for C₁₄H₁₆BrN₂O₂: 323.0390; found: 323.0388.

4.1.1.13.

8-Bromo-10-chloro-2-methyl-1,11b-dihydro-pyrazolo[1,5-d][1,4]benzoxazepin-5(6H)-one (3m). White powder, yield, 15%; m.p. 218–221°C; ¹H NMR (300 MHz, CDCl₃) δ 7.61 (d, $J = 2.3$ Hz, 1H), 7.18 (d, $J = 2.1$ Hz, 1H), 5.83 (dd, $J = 11.2, 9.0$ Hz, 1H, 11b-H), 4.99 (d, $J = 16.8$ Hz, 1H, 6-Hb), 4.44 (d, $J = 16.8$ Hz, 1H, 6-Ha), 3.42 (dd, $J = 18.1, 8.9$ Hz, 1H, 1-Hb), 3.27 (dd, $J = 18.0, 11.3$ Hz, 1H, 1-Ha), 2.22 (s, 3H, 2-CH₃); ¹³C NMR (75 MHz, CDCl₃) δ 163.5, 157.7, 153.4, 134.4, 133.4, 131.3, 124.3, 117.4, 71.6 (C-6), 55.9 (11b-C), 39.5 (C-1), 16.2 (2-CH₃). TOF-HRMS: m/z [M + H]⁺ calcd for C₁₂H₁₁BrClN₂O₂: 328.9687; found: 328.9692.

4.1.1.14.

8-Bromo-10-chloro-2-methyl-6-methyl-1,11b-dihydro-pyrazolo[1,5-d][1,4]benzoxazepin-5(6H)-one (3n). White powder, yield, 16%; m.p. 205–207°C; ¹H NMR (300 MHz, CDCl₃) δ 7.58 (d, $J = 2.3$ Hz, 1H), 7.12 (d, $J = 2.2$ Hz, 1H), 5.68 (t, $J = 10.6$ Hz, 1H), 5.08 (q, $J = 6.9$ Hz, 1H, 6-Hb), 3.34 (d, $J = 10.6$ Hz, 2H, 1-H), 2.20 (s, 3H, 2-CH₃), 1.61 (d, $J = 6.9$

Hz, 3H, 6-CH₃); ¹³C NMR (75 MHz, CDCl₃) δ 166.60, 157.9, 151.5, 133.2, 131.9, 129.5, 125.7, 118.1, 78.2 (C-6), 57.5 (11b-C), 42.3 (C-1), 17.4 (6-CH₃), 16.2 (2-CH₃). TOF-HRMS: *m/z* [M + H]⁺ calcd for C₁₃H₁₃BrClN₂O₂: 342.9843; found: 342.9847.

4.1.1.15.

8-Bromo-10-chloro-6-ethyl-2-methyl-1,11b-dihydro-pyrazolo[1,5-d][1,4]benzoxazepin-5(6H)-one (3o). White powder, yield, 14%; m.p. 227–229°C; ¹H NMR (300 MHz, CDCl₃) δ 7.52 (dd, *J* = 2.4, 0.5 Hz, 1H), 7.01 (dd, *J* = 2.4, 0.8 Hz, 1H), 5.72 (dd, *J* = 10.9, 10.3 Hz, 1H, 11b-H), 4.56 (dd, *J* = 7.5, 5.5 Hz, 1H, 6-Ha), 3.52 (dd, *J* = 17.5, 11.2 Hz, 1H, 1-Hb), 3.23 (dd, *J* = 16.8, 10.0 Hz, 1H, 1-Ha), 2.15 (s, 3H, 2-CH₃), 2.13–2.03 (m, 2H, 6-CH₂CH₃), 1.15 (t, *J* = 7.4 Hz, 3H, 6-CH₂CH₃); ¹³C NMR (75 MHz, CDCl₃) δ 165.8, 157.8, 152.6, 132.8, 128.8, 127.8, 126.8, 115.9, 81.40 (C-6), 58.76 (11b-C), 45.3 (C-1), 23.9 (6-CH₂CH₃), 16.1 (2-CH₃), 10.3 (6-CH₂CH₃). TOF-HRMS: *m/z* [M + H]⁺ calcd for C₁₄H₁₅BrClN₂O₂: 342.9843; found: 342.9847.

4.1.1.16.

8-Methoxy-2-methyl-1,11b-dihydro-pyrazolo[1,5-d][1,4]benzoxazepin-5(6H)-one (3p). White powder, yield, 19%; m.p. 180–182°C; ¹H NMR (300 MHz, CDCl₃) δ 7.17 (t, *J* = 8.0 Hz, 1H), 6.99 (d, *J* = 8.1 Hz, 1H), 6.83 (d, *J* = 7.8 Hz, 1H), 5.95–.82 (m, 1H, 11b-H), 4.99 (d, *J* = 16.8 Hz, 1H, 6-Hb), 4.40 (d, *J* = 16.8 Hz, 1H, 6-Ha), 3.90 (s, 3H, OCH₃), 3.49 (dd, *J* = 18.0, 9.0 Hz, 1H, 1-Hb), 3.22 (dd, *J* = 18.0, 11.4 Hz, 1H, 1-Ha), 2.21 (s, 3H, 2-CH₃). TOF-HRMS: *m/z* [M + H]⁺ calcd for C₁₃H₁₅N₂O₃: 247.1077; found: 247.1085.

4.1.1.17.

8-Methoxy-2-methyl-6-methyl-1,11b-dihydro-pyrazolo[1,5-d][1,4]benzoxazepin-5(6H)-one (3q). White powder, yield, 19%; m.p. 172–174°C; ¹H NMR (300 MHz, CDCl₃) δ 7.14 (t, *J* = 8.0 Hz, 1H), 6.97 (d, *J* = 8.2 Hz, 1H), 6.82 (d, *J* = 7.8 Hz, 1H), 5.76 (t, *J* = 10.7 Hz, 1H, 11b-H), 5.13 (q, *J* = 7.1 Hz, 1H, 6-Hb), 3.88 (s, 3H, OCH₃), 3.45 (dd, *J* = 17.7, 10.4 Hz, 1H, 1-Hb), 3.22 (dd, *J* = 17.6, 11.2 Hz, 1H, 1-Ha), 2.20 (s, 3H, 2-CH₃), 1.50 (d, *J* = 7.0 Hz, 3H, 6-CH₃). TOF-HRMS: *m/z* [M + H]⁺ calcd for C₁₄H₁₇N₂O₃: 261.1234; found: 261.1244.

4.1.1.18.

2-Methyl-10-methyl-1,11b-dihydro-pyrazolo[1,5-d][1,4]benzoxazepin-5(6H)-one (**3r**).

White powder, yield, 21%; m.p. 176–178°C; ¹H NMR (300 MHz, CDCl₃) δ 7.17 (d, *J* = 8.1 Hz, 1H), 7.07 (d, *J* = 8.1 Hz, 1H), 7.02 (s, 1H), 5.89 – 5.74 (m, 1H, 11b-H), 4.95 (d, *J* = 16.7 Hz, 1H, 6-Hb), 4.37 (d, *J* = 16.7 Hz, 1H, 6-Ha), 3.51 (dd, *J* = 17.9, 9.5 Hz, 1H, 1-Hb), 3.21 (dd, *J* = 17.9, 11.3 Hz, 1H, 1-Ha), 2.36 (s, 3H, 10-CH₃), 2.22 (s, 3H, 2-CH₃). TOF-HRMS: *m/z* [M + H]⁺ calcd for C₁₃H₁₅N₂O₂: 231.1128; found: 231.1123.

4.1.1.19.

2-Methyl-6-methyl-10-methyl-1,11b-dihydro-pyrazolo[1,5-d][1,4]benzoxazepin-5(6H)-one (**3s**).

White powder, yield, 20%; m.p. 146–148°C; ¹H NMR (300 MHz, CDCl₃) δ 7.09 (d, *J* = 8.1 Hz, 1H), 6.94 (d, *J* = 8.2 Hz, 2H), 5.75 (t, *J* = 10.6 Hz, 1H, 11b-H), 4.96 (q, *J* = 6.9 Hz, 1H, 6-Hb), 3.42 (dd, *J* = 17.8, 10.1 Hz, 1H, 1-Hb), 3.30 (dd, *J* = 17.4, 11.0 Hz, 1H, 1-Ha), 2.34 (s, 3H, 10-CH₃), 2.18 (s, 3H, 2-CH₃), 1.49 (d, *J* = 6.9 Hz, 3H, 6-CH₃); ¹³C NMR (75 MHz, CDCl₃) δ 167.5, 158.0, 152.9, 133.7, 130.1, 129.0, 126.4, 122.7, 76.4 (C-6), 57.7 (11b-C), 42.0 (C-1), 21.2 (10-CH₃), 17.7 (6-CH₃), 16.3 (2-CH₃). TOF-HRMS: *m/z* [M + H]⁺ calcd for C₁₄H₁₇N₂O₂: 245.1285; found: 245.1291.

4.1.2. General procedure for the preparation of compounds **3t–3x**

To a solution of aromatic methyl ketones (10 mmol) and salicylaldehyde (11 mmol) in ethanol (20 mL) was added 40% NaOH solution (2 mL) dropwise and the reaction was carried out at 60 °C for 5 h. The mixture was poured into cold water and neutralized with 2 M HCl to a pH in the range of 5–6. The resulting precipitate was collected, washed with water and dried to give chalcones. The chalcone was treated with 5 times excess of hydrazine hydrate in ethanol and refluxed for 5 h. The reaction mixture was then poured into ice-cold water. The solid was filtered, washed and recrystallized from ethanol to afford respective pyrazoline (**1**). A solution of compound **1** in CH₂Cl₂ (20 mL) was added α-bromoacyl chloride (4.0 mmol) and 4-dimethylaminopyridine (5.0 mmol) and the reaction was stirred overnight. The reaction mixture was washed with water and brine, dried with anhydrous Na₂SO₄, filtrated and concentrated *in vacuo*. The resulting residue

was then purified by column chromatography to give product **2**. NaHCO₃ (3.0 mmol) was added to an ethanol (20 mL) solution of compound **2** (2.0 mmol), then the reaction mixture was stirred at 70 °C until the disappearance of starting material (monitored by TLC). EtOAc (100 mL) was added to the reaction mixture, then washed with water and brine, dried with anhydrous Na₂SO₄, filtrated and concentrated in vacuo. The residue was purified by column chromatography (petroleum/EtOAc, 1:1 → 1:2) to give title compounds **3t–3x**.

4.1.2.1. *10-Bromo-2-furan-1,11b-dihydro-pyrazolo[1,5-d][1,4]benzoxazepin-5(6H)-one (3t)*. White powder, yield, 13%; m.p. 213–215°C; ¹H NMR (300 MHz, CDCl₃) δ 7.60 (d, *J* = 1.5 Hz, 1H, Fu-H), 7.52 (dd, *J* = 8.5, 2.2 Hz, 1H, Ar-H), 7.43 (d, *J* = 1.8 Hz, 1H, Fu-H), 7.16–7.05 (m, 2H, Ar-H), 6.58 (dd, *J* = 3.5, 1.7 Hz, 1H, Fu-H), 5.99–.85 (m, 1H, 11b-H), 5.02 (d, *J* = 16.7 Hz, 1H, 6-Hb), 4.45 (d, *J* = 16.6 Hz, 1H, 6-Ha), 3.83 (dd, *J* = 17.7, 9.3 Hz, 1H, 1-Hb), 3.67 (dd, *J* = 17.7, 11.5 Hz, 1H, 1-Ha); ¹³C NMR (75 MHz, CDCl₃) δ 164.2, 157.0, 147.8, 146.3, 145.2, 133.6, 132.7, 128.1, 123.3, 118.2, 113.4, 112.5, 72.8 (C-6), 55.5 (11b-H), 35.4 (C-1). TOF-HRMS: *m/z* [M + H]⁺ calcd for C₁₅H₁₂BrN₂O₃: 347.0026; found: 347.0029.

4.1.2.2.

8,10-Dichloro-2-furan-6-methyl-1,11b-dihydro-pyrazolo[1,5-d][1,4]benzoxazepin-5(6H)-one (3u). White powder, yield, 15%; m.p. 249–253°C; ¹H NMR (300 MHz, CDCl₃) δ 7.58 (s, 1H, Fu-H), 7.45 (d, *J* = 2.1 Hz, 1H, Ar-H), 7.17 (s, 1H, Fu-H), 7.09 (d, *J* = 3.4 Hz, 1H, Ar-H), 6.62 – 6.53 (m, 1H, Fu-H), 5.81 (t, *J* = 10.7 Hz, 1H, 11b-H), 5.17 (q, *J* = 7.0 Hz, 1H, 6-Hb), 3.74 (dd, *J* = 10.7, 3.4 Hz, 2H, 1-H), 1.62 (d, *J* = 7.0 Hz, 3H, 6-CH₃). TOF-HRMS: *m/z* [M + H]⁺ calcd for C₁₆H₁₃Cl₂N₂O₃: 351.0298; found: 351.0302.

4.1.2.3.

8,10-Dibromo-2-(4-fluoro-phenyl)-1,11b-dihydro-pyrazolo[1,5-d][1,4]benzoxazepin-5(6H)-one (3v). White powder, yield, 12%; m.p. 276–279°C; ¹H NMR (300 MHz, CDCl₃) δ 7.91 (dd, *J* = 7.7, 5.4 Hz, 2H), 7.79 (s, 1H), 7.39 (s, 1H), 7.16 (t, *J* = 8.2 Hz, 2H), 6.09–5.93 (m, 1H, 11b-H), 5.06 (d, *J* = 16.8 Hz, 1H, 6-Hb), 4.50 (d, *J* = 16.8 Hz, 1H,

6-Ha), 3.80 (dd, $J = 17.5, 8.9$ Hz, 1H, 1-Hb), 3.69 (dd, $J = 17.6, 11.5$ Hz, 1H, 1-Ha); ^{13}C NMR (75 MHz, CDCl_3) δ 163.8, 154.9, 153.9, 136.4, 134.6, 129.7, 127.2, 126.7, 118.7, 117.8, 116.4, 116.1, 71.8 (C-6), 56.4 (11b-H), 35.6 (C-1). TOF-HRMS: m/z $[\text{M} + \text{Na}]^+$ calcd for $\text{C}_{17}\text{H}_{11}\text{Br}_2\text{FN}_2\text{NaO}_2$: 474.9064; found: 474.9066.

4.1.2.4.

10-Bromo-2-(4-fluoro-phenyl)-1,11b-dihydro-pyrazolo[1,5-d][1,4]benzoxazepin-5(6H)-one (3w). White powder, yield, 14%; m.p. 181–184°C; ^1H NMR (300 MHz, CDCl_3) δ 7.97–7.83 (m, 2H), 7.52 (dd, $J = 8.5, 2.2$ Hz, 1H), 7.44 (s, 1H), 7.21–6.92 (m, 3H), 6.05–5.89 (m, 1H, 11b-H), 5.03 (d, $J = 16.7$ Hz, 1H, 6-Hb), 4.47 (d, $J = 16.7$ Hz, 1H, 6-Ha), 3.82 (dd, $J = 17.4, 9.3$ Hz, 1H, 1-Hb), 3.68 (dd, $J = 17.4, 11.5$ Hz, 1H, 1-Ha). TOF-HRMS: m/z $[\text{M} + \text{H}]^+$ calcd for $\text{C}_{17}\text{H}_{13}\text{BrFN}_2\text{O}_2$: 375.0139; found: 375.0130.

4.1.2.5.

10-Chloro-2-(4-fluoro-phenyl)-1,11b-dihydro-pyrazolo[1,5-d][1,4]benzoxazepin-5(6H)-one (3x). White powder, yield, 12%; m.p. 209–211°C; ^1H NMR (300 MHz, CDCl_3) δ 7.99–7.86 (m, 2H), 7.42–7.27 (m, 2H), 7.15 (t, $J = 8.7$ Hz, 3H), 6.03–5.89 (m, 1H, 11b-H), 5.02 (d, $J = 16.7$ Hz, 1H, 6-Hb), 4.45 (d, $J = 16.7$ Hz, 1H, 6-Ha), 3.82 (dd, $J = 17.4, 9.3$ Hz, 1H, 1-Hb), 3.68 (dd, $J = 17.4, 11.5$ Hz, 1H, 1-Ha). TOF-HRMS: m/z $[\text{M} + \text{H}]^+$ calcd for $\text{C}_{17}\text{H}_{13}\text{ClFN}_2\text{O}_2$: 331.0644; found: 331.0650.

4.1.3. General procedure for the preparation of compounds (6R)-3o and (6S)-3o

To a CH_2Cl_2 (5 mL) solution of 2-bromo-4-chloro-6-(3-methyl-4,5-dihydro-1H-pyrazol-5-yl)phenol (150 mg, 0.52 mmol) was added 2-chloropropionic acid (67 mg, 0.55 mmol), EDC·HCl (195 mg, 1.0 mmol) and HOBt (135 mg, 1.0 mmol), the mixture was stirred 30 min at room temperature. After NEt_3 (140 μL) was added, the reaction solution was stirred overnight. The mixture was washed twice with water, dried with Na_2SO_4 , filtered, and concentrated *in vacuo*. The residue was dissolved in ethanol (10 mL), NaHCO_3 (84 mg, 1.0 mmol) was added to the solution. The reaction mixture was stirred at 60–70 °C until the disappearance of starting material (TLC monitoring). EtOAc (100 mL) was added to the reaction mixture,

then washed with water and brine, dried with anhydrous Na_2SO_4 , filtrated and concentrated *in vacuo*. The residue was purified by column chromatography (petroleum/EtOAc, 1:1 \rightarrow 1:3) to give enantiomers (**6R**)-**3o** and (**6S**)-**3o**.

4.1.3.1.

8-Bromo-10-chloro-6R-ethyl-2-methyl-1,11b-dihydro-pyrazolo[1,5-d][1,4]benzoxazepin-5(6H)-one ((6R)-3o). White powder, yield, 32%; $[\alpha]_D^{20} = -202^\circ$ ($c = 0.164$, CHCl_3); m.p. 219–221°C; $^1\text{H NMR}$ (600 MHz, CDCl_3) δ 7.51 (d, $J = 1.8$ Hz, 1H), 7.00 (s, 1H), 5.71 (t, $J = 10.6$ Hz, 1H, 11b-H), 4.55 (dd, $J = 8.1, 4.9$ Hz, 1H, 6-Ha), 3.52 (dd, $J = 17.5, 11.2$ Hz, 1H, 1-Hb), 3.22 (dd, $J = 17.4, 10.0$ Hz, 1H, 1-Ha), 2.15 (s, 3H, 2- CH_3), 2.13–2.03 (m, 2H, 6- CH_2CH_3), 1.13 (t, $J = 7.4$ Hz, 3H, 6- CH_2CH_3).

4.1.3.2.

8-Bromo-10-chloro-6S-ethyl-2-methyl-1,11b-dihydro-pyrazolo[1,5-d][1,4]benzoxazepin-5(6H)-one ((6S)-3o). White powder, yield, 34%; $[\alpha]_D^{20} = +167^\circ$ ($c = 0.154$, CHCl_3); m.p. 215–218°C; $^1\text{H NMR}$ (600 MHz, CDCl_3) δ 7.5c2 (d, $J = 2.0$ Hz, 1H), 7.00 (s, 1H), 5.71 (t, $J = 10.6$ Hz, 1H, 11b-H), 4.55 (dd, $J = 8.2, 4.9$ Hz, 1H, 6-Ha), 3.56 – 3.47 (m, 1H, 1-Hb), 3.22 (dd, $J = 17.5, 10.0$ Hz, 1H, 1-Ha), 2.15 (s, 3H, 2- CH_3), 2.13–2.03 (m, 2H, 6- CH_2CH_3), 1.13 (t, $J = 7.4$ Hz, 3H, 6- CH_2CH_3).

4.2. EeAChE and eqBuChE inhibition assays

Enzymatic inhibition assays were performed on AChE from electric eel (C3389-500UN; Sigma) and BuChE from equine serum (C4290-1KU; Sigma), according to the spectrophotometric Ellman's method as previously described. The experiment was performed in 48-well plates in a final volume of 500 μL . Each well contained 0.036 U/mL of EeAChE or eqBuChE, and 0.1 M pH 8 phosphate buffer. They were preincubated for 20 min at different compound concentrations at 37 °C. Then 0.35 mM acetylthiocholine iodide (ATCh; A5751-1G; Sigma) or 0.5 mM butyrylthiocholine iodide (20820-1G; Sigma) and 0.35 mM 5,5'-ditiobis-2-nitrobenzoico (DTNB; D8130-1G;

Sigma) were added. The DTNB produces the yellow anion 5-thio-2-nitrobenzoic acid along with the enzymatic degradation of acetylthiocholine or butyrylthiocholine. Changes in absorbance were measured at 410 nm after 20 min in a Biotek Synergy HTX Multi-Mode reader. The IC₅₀ values were determined graphically from inhibition curves (log inhibitor concentration vs percent of inhibition). A control experiment was performed under the same conditions without inhibitor and the blank contained buffer, DMSO, DTNB, and substrate.

4.3. Oil/water partition coefficient assessment and ADMET prediction

Octanol–water partition coefficients of title compounds were measured by the shake flask method with slight modification. The aqueous phase was replaced by PBS (pH = 7.4). Both the octanol and the aqueous phase were saturated with each other before use. The assay mixture containing test compounds was shaken at 37 °C. After 24 h, the mixture was centrifuged at 4000 rpm for 30 min, followed by the measured with ultraviolet spectrophotometer. The logP values were calculated.

The active compounds were analyzed with the ADMET prediction tools of DS 2017R2. The pharmacokinetic properties are HIA (human intestinal absorption), PPB (plasma protein binding), Cytochrome P450 2D6 binding (CYP2D6), Aqueous solubility, and BBB. ADMET screening in a stepwise manner is summarized as follows. HIA: there are four prediction levels of 0–3 represent good, moderate, low, and very low absorption respectively. The data displayed that these compounds all had good absorption (HIA levels of 0, score < 6.126). Aqueous solubility: solubility levels of 0–5 represent extremely low; no, very low, but possible; yes, low; yes, good; yes, optimal; no, too soluble respectively, and we found these compounds have good solubility (solubility level of 2 and 3). BBB: BBB levels of 0–4 represent very high, high, medium, low, and undefined penetration respectively. The results showed that four compounds had high penetrant and three compounds had medium penetrant. CYP2D6 binding activity: CYP2D6 is involved in the metabolism of a wide range of substrates in the liver and its inhibition by a drug constitutes a major of drug-drug interaction. The level of 0 and 1 reflect as non-inhibitor and inhibitor. The results showed that active compounds were non-inhibitors of CYP2D6 (CYP2D6 level of 0). PPB: PPB levels of 0, 1, and 2 reflect

on binding as < 90%, binding as > 90%, and binding as > 95%. Based on PSA2D and ALogP98 standard, the active compounds were found to fulfill the set standard at both 95% and 99% confidence limit ellipses for the BBB penetration and HIA models, respectively, in conformity with the data presented.

4.3. Cytotoxicity Assays

PC12 cells were cultured in DMEM containing 10% fetal bovine serum, 100 units/mL penicillin, and 100 µg/mL streptomycin at 37 °C in a 5% CO₂ humidify atmosphere. Cell cytotoxicity was evaluated by methyl thiazolyl tetrazolium (MTT) assay. PC12 cells were inoculated at 1×10^4 cells per well in 96-well plate. After cultured for 24 h, the cells were treated with different compounds which were diluted in DMEM for 24 h. Then 20 µL of 0.5 mg/mL MTT reagent was added into the cells and incubated for 4 h. After 4 h, cell culture was removed and then 150 µL DMSO was added to dissolve the formazan. The optical density was measured at 570 nm (OD₅₇₀). Cell viability was calculated from three independent experiments. The density of formazan formed in blank group was set as 100% of viability. Cell viability (%) = compound (OD₅₇₀ / blank (OD₅₇₀) × 100%

Blank: cultured with fresh medium only.

Compound: treated with compounds or donepezil.

4.4. Neuroprotection assay

Neuroprotective activity was evaluated as described in the literature. Differentiated PC12 cells were incubated with different concentrations of the compound **3o** for 3 h before treatment with H₂O₂ (300 µM). Cell viability was measured after 24 h by using the MTT assay. Briefly, 20 µL of 0.5 mg/mL MTT reagent was added into the cells and incubated for 4 h. After 4 h, cell culture was removed and then 150 µL DMSO was added to dissolve the formazan. The optical density was measured at 570 nm (OD₅₇₀) on the Biotek Synergy HTX Multi-Mode reader. Results were adjusted considering OD measured in the blank.

4.5. Kinetic studies of eqBuChE inhibition

Kinetic studies were performed with the same test conditions, using six concentrations of substrate (from 0.1 to 1 mM) and four concentrations of inhibitor (0–20 μ M). Apparent inhibition constants and kinetic parameters were calculated within the “Enzyme kinetics” module of Prism 5.

4.6. Molecular docking study

A structure based in silico procedure was applied to discover the binding modes of the active compounds to BuChE enzyme active site. The CDOCKER of Discovery Studio 2017R2 (DS) was conducted to explain SAR of series compounds and further guide the design of more effective and concrete BuChE inhibitors. The ligand binding to the crystal structure of hBuChE with PDB ID: 1P0I was selected as template. The target enzyme was prepared with Prepare Protein of DS to ensure the integrity of target. The ligand was processed by Full Minimization of the Small Molecular in DS. Then the title compounds were docked into the active site of protein using CDOCKER. The view results of molecular docking were extracted after the program running end, each docking result was analyzed for interaction and their different pose. The binding energies of most potent compounds were clearly observed and tabulated in Table 3. The lowest -CDOCKER_INTERACTION_ENERGY values of those poses were regarded as the most stable and picked to analysis binding interactions with target enzyme visualized.

Acknowledgments

Financial support was provided by the National Natural Science Funding of China (21572003, 20802003), Anhui University Natural Science Research Project (KJ2016A339), and University Project of Introduction and Cultivation of Leading Talents (gxfxZD2016044).

Notes

The authors declare no competing financial interest.

BuChE, butyrylcholinesterase; AChE, acetylcholinesterase; AD, Alzheimer's disease; ADMET, absorption, distribution, metabolism, excretion and toxicity in pharmacokinetics; ChE, cholinesterase; PD, Parkinson disease; MAO, monoamine oxidase; EeAChE, *Electrophorus electricus* AChE; eqBuChE, equine BuChE; AChEIs, AChE inhibitors; BBB, blood-brain barrier; HIA, human intestinal absorption; PPB, plasma protein binding; CYP2D6, Cytochrome P450 2D6.

Appendix A. Supplementary material

Representative ^1H and ^{13}C NMR spectra can be found at <http://>

References

- [1] H.W. Querfurth, F.M. LaFerla, Alzheimer's disease, *N. Engl. J. Med.* 362 (2010) 329–344.
- [2] M. Prince, A. Comas-Herrera, M. Knapp, M. Guerchet, M. Karagiannidou, *Alzheimer's Disease International*, 2016.
- [3] C.L. Masters, D.J. Selkoe, Biochemistry of amyloid β -protein and amyloid deposits in Alzheimer Disease, *Cold Spring Harbor Perspect. Med.* 2 (2012) a006262.
- [4] J. Avila, Tau phosphorylation and aggregation in Alzheimer's disease pathology, *FEBS Lett.* 580 (2006) 2922–2927.
- [5] M.L. Müller, N.I. Bohnen, Cholinergic dysfunction in Parkinson's disease, *Curr. Neurol. Neurosci. Rep.* 13 (2013) 377.
- [6] M. Rosini, E. Simoni, A. Milelli, A. Minarini, C. Melchiorre, Oxidative stress in Alzheimer's disease: are we connecting the dots? *J. Med. Chem.* 57 (2014) 2821–2831.
- [7] P. Scheltens, K. Blennow, M.M. Breteler, B de Strooper, GB Frisoni, S. Salloway, W.M. Van der Flier, Alzheimer's disease. *Lancet* 388 (2016) 505–517.
- [8] R.T. Bartus, R.L. Dean, B. Beer, A.S. Lippa, The cholinergic hypothesis of geriatric memory dysfunction, *Science* 217 (1982) 408–414.
- [9] D. Zhou, W. Zhou, J.K. Song, Z.Y. Feng, R.Y. Yang, S. Wu, L. Wang, A.L. Liu, G.H. Du, DL0410, a novel dual cholinesterase inhibitor, protects mouse brains against A β -induced neuronal damage via the Akt/JNK signaling pathway, *Acta Pharmacol. Sin.*

37 (2016) 1401–1412.

[10] C. Grantham, H. Geerts, The rationale behind cholinergic drug treatment for dementia related to cerebrovascular disease, *J. Neurol. Sci.* 203-204 (2002) 131–136.

[11] E. Perry, M. Walker, J. Grace, R. Perry, Acetylcholine in mind: a neurotransmitter correlate of consciousness? *Trends Neurosci.* 22 (1999) 273–280.

[12] E. Giacobini, R. Spiegel, A. Enz, A. Veroff, N. Cutler, Inhibition of acetyl- and butyryl-cholinesterase in the cerebrospinal fluid of patients with Alzheimer's disease by rivastigmine: correlation with cognitive benefit, *J. Neural Transm.* 109 (2002) 1053–1065.

[13] G. Mushtaq, N.H. Greig, J.A. Khan, M.A. Kamal, Status of acetylcholinesterase and butyrylcholinesterase in Alzheimer's disease and type 2 diabetes mellitus, *CNS Neurol. Disord. Drug Targets* 13 (2014) 1432–1439.

[14] R.M. Lane, S.G. Potkin, A. Enz, Targeting acetylcholinesterase and butyrylcholinesterase in dementia, *Int. J. Neuropsychopharmacol.* 9 (2006) 101–124.

[15] S.F. McHardy, H.L. Wang, S.V. McCowen, M.C. Valdez, Recent advances in acetylcholinesterase Inhibitors and Reactivators: an update on the patent literature (2012-2015), *Expert. Opin. Ther. Pat.* 27 (2017) 455–476.

[16] E. Perry, R. Perry, G. Blessed, B. Tomlinson, Changes in brain cholinesterases in senile dementia of Alzheimer type, *Neuropathol. Appl. Neurobiol.* 4 (1978) 273–277.

[17] X. Norel, M. Angrisani, C. Labat, I. Gorenne, E. Dulmet, F. Rossi, C. Brink, Degradation of acetylcholine in human airways: role of butyrylcholinesterase, *Br. J. Pharmacol.* 108 (1993) 914–919.

[18] J. Hartmann, C. Kiewert, E.G. Duysen, O. Lockridge, N.H. Greig, J. Klein, Excessive hippocampal acetylcholine levels in acetylcholinesterase-deficient mice are moderated by butyrylcholinesterase activity, *J. Neurochem.* 100 (2007) 1421–1429.

[19] N.H. Greig, T. Utsuki, D.K. Ingram, Y. Wang, G. Pepeu, C. Scali, Q.-S. Yu, J. Mamczarz, H.W. Holloway, T. Giordano, Selective butyrylcholinesterase inhibition elevates brain acetylcholine, augments learning and lowers Alzheimer β -amyloid peptide in rodent, *Proc. Natl. Acad. Sci. U. S. A.* 102 (2005) 17213–17218.

[20] F.H. Darras, B. Kling, E. Sawatzky, J. Heilmann, M. Decker, Cyclic acyl guanidines bearing carbamate moieties allow potent and dirigible cholinesterase inhibition of either

- acetyl- or butyrylcholinesterase, *Bioorg, Med, Chem.* 22 (2014) 5020–5034.
- [21] V.P. Chen, Y. Gao, L. Geng, R. J. Parks, Y.-P. Pang, S. Brimijoin, Plasma butyrylcholinesterase regulates ghrelin to control aggression, *Proc. Natl. Acad. Sci. U. S. A.* 112 (2015) 2251–2256.
- [22] R. Csuk, S. Albert, R. Kluge, D. Strohl, Resveratrol derived butyrylcholinesterase inhibitors, *Arch. Pharm.* 346 (2013) 499-503.
- [23] Q. Li, H. Yang, Y. Chen, H. Sun, Recent progress in the identification of selective butyrylcholinesterase inhibitors for Alzheimer's disease, *Eur. J. Med. Chem.* 132 (2017) 294–309.
- [24] R. Otto, R. Penzis, F. Gaube, O. Adolph, K.J. Fohr, P. Warncke, D. Robaa, D. Appenroth, C. Fleck, C. Enzensperger, J. Lehmann, T. Winckler, Evaluation of homobivalent carbolines as designed multiple ligands for the treatment of neurodegenerative disorders, *J. Med. Chem.* 58 (2015) 6710–6715.
- [25] O. Di Pietro, F.J. Pérez-Areales, J. Juárez-Jiménez, A. Espargaró, M.V. Clos, B. Pérez, R. Lavilla, R. Sabaté, F.J. Luque, D. Muñoz-Torrero, Tetrahydrobenzo[h][1,6]naphthyridine-6-chlorotacrine hybrids as a new family of anti-Alzheimer agents targeting β -Amyloid, Tau, and cholinesterase pathologies, *Eur. J. Med. Chem.* 84 (2014) 107–117.
- [26] S. Montanari, L. Scalvini, M. Bartolini, F. Belluti, S. Gobbi, V. Andrisano, A. Ligresti, V. Di Marzo, S. Rivara, M. Mor, A. Bisi, A. Rampa, Fatty acid amide hydrolase (FAAH), acetylcholinesterase (AChE), and butyrylcholinesterase (BuChE): Networked targets for the development of carbamates as potential anti-Alzheimer's disease agents, *J. Med. Chem.* 59 (2016) 6387–6406.
- [27] M.Y. Wu, G. Esteban, S. Brogi, M. Shionoya, L. Wang, G. Campiani, M. Unzeta, T. Inokuchi, S. Butini, J. Marco-Contelles, Donepezil-like multifunctional agents: Design, synthesis, molecular modeling and biological evaluation, *Eur. J. Med. Chem.* 121 (2016) 864–879.
- [28] D. Palanimuthu, R. Poon, S. Sahni, R. Anjum, D. Hibbs, H.Y. Lin, P.V. Bernhardt, D.S. Kalinowski, D.R. Richardson, A novel class of thiosemicarbazones show multi-functional activity for the treatment of Alzheimer's disease, *Eur. J. Med. Chem.* 139 (2017) 612–632.

- [29] J. Hroudová, N. Singh, Z. Fišar, K.K. Ghosh, Progress in drug development for Alzheimer's disease: An overview in relation to mitochondrial energy metabolism, *Eur. J. Med. Chem.* 121 (2016) 774–784.
- [30] J. Sterling, Y. Herzig, T. Goren, N. Finkelstein, D. Lerner, W. Goldenberg, I. Miskolczi, S. Molnar, F. Rantal, T. Tamas, G. Toth, A. Zagyva, A. Zekany, G. Lavian, A. Gross, R. Friedman, M. Razin, W. Huang, B. Kraiss, M. Chorev, M.B.H. Youdim, M. Weinstock, Novel dual inhibitors of AChE and MAO derived from hydroxy aminoindan and phenethylamine as potential treatment for Alzheimer's disease, *J. Med. Chem.* 45 (2002) 5260–5279.
- [31] R. Farina, L. Pisani, M. Catto, O. Nicolotti, D. Gadaleta, N. Denora, R. Soto-Otero, E. Mendez-Alvarez, C.S. Passos, G. Muncipinto, C.D. Altomare, A. Nurisso, P.A. Carrupt, A. Carotti, Structure-based design and optimization of multitarget-directed 2H-Chromen-2-one derivatives as potent inhibitors of monoamine oxidase B and cholinesterases, *J. Med. Chem.* 58 (2015) 5561–5578.
- [32] L. Pisani, R. Farina, M. Catto, R.M. Iacobazzi, O. Nicolotti, S. Cellamare, G.F. Mangiatordi, N. Denora, R. Soto-Otero, L. Siragusa, C.D. Altomare, A. Carotti, Exploring basic tail modifications of coumarin-based dual acetylcholinesterase-monoamine oxidase B inhibitors: Identification of water-soluble, brain-permeant neuroprotective multitarget agents, *J. Med. Chem.* 59 (2016) 6791–6806.
- [33] X. Tong, R. Chen, T.T. Zhang, Y. Han, W.J. Tang, X.H. Liu, Design and synthesis of novel 2-pyrazoline-1-ethanone derivatives as selective MAO inhibitors, *Bioorg. Med. Chem.* 23 (2015) 515–525.
- [34] R. Chen, J. Xiao, Y. Ni, H.F. Xu, M. Zheng, X. Tong, T.T. Zhang, C. Liao, W.J. Tang, Novel tricyclic pyrazolo[1,5-d][1,4]benzoxazepin-5(6H)-one: Design, synthesis, model and use as hMAO-B inhibitors, *Bioorg. Med. Chem.* 24 (2016) 1741–1748.
- [35] M.B. Youdim, D. Edmondson, K.F. Tipton, The therapeutic potential of monoamine oxidase inhibitors, *Nat. Rev. Neurosci.* 7 (2006) 295–309.
- [36] M. Naoi, W. Maruyama, K. Inaba-Hasegawa, Type A and B monoamine oxidase in age-related neurodegenerative disorders: their distinct roles in neuronal death and survival, *Curr. Top. Med. Chem.* 12 (2012) 2177–2188.
- [37] G.L. Ellman, K.D. Courtney, V. Andres, R.M. Featherstone, A new and rapid

colorimetric determination of acetylcholinesterase activity, *Biochem. Pharmacol.* 7 (1961) 88–95.

[38] H. Sugimoto, Y. Limura, Y. Yamanishi, K. Yamatsu, Synthesis and structure-activity relationships of acetylcholinesterase inhibitors: 1-benzyl-4-[(5,6-dimethoxy-1-oxoindan-2-yl)methyl]piperidine hydrochloride and related compounds, *J. Med. Chem.* 38 (1995) 4821–4829.

[39] M. Bartolini, C. Bertucci, V. Cavrini, V. Andrisano, beta-Amyloid aggregation induced by human acetylcholinesterase: inhibition studies, *Biochem. Pharmacol.* 65 (2003) 407–416.

[40] E. Tamagno, P. Bardini, A. Obbili, A. Vitali, R. Borghi, D. Zaccheo, M.A. Pronzato, O. Danni, M.A. Smith, G. Perry, M. Tabaton, Oxidative stress increases expression and activity of BACE in NT2 neurons, *Neurobiol. Dis.* 10 (2002) 279–288.

[41] Z. Najafi, M. Mahdavi, M. Saeedi, E. Karimpour-Razkenari, R. Asatouri, F. Vafadarnejad, F.H. Moghadam, M. Khanavi, M. Sharifzadeh, T. Akbarzadeh, Novel tacrine-1,2,3-triazole hybrids: In vitro, in vivo biological evaluation and docking study of cholinesterase inhibitors, *Eur. J. Med. Chem.* 125 (2017) 1200–1212.

[42] X. Zha, D. Lamba, L. Zhang, Y. Lou, C. Xu, D. Kang, L. Chen, Y. Xu, L. Zhang, A. De Simone, S. Samez, A. Pesaresi, J. Stojan, M.G. Lopez, J. Egea, V. Andrisano, M. Bartolini, Novel tacrine-benzofuran hybrids as potent multitarget-directed ligands for the treatment of Alzheimer's disease: Design, synthesis, biological evaluation, and X-ray crystallography, *J. Med. Chem.* 59 (2016) 114–131.

[43] W.J. Tang, J. Wang, X. Tong, J.B. Shi, X.H. Liu, J. Li, Design and synthesis of celastrol derivatives as anticancer agents, *Eur. J. Med. Chem.* 95 (2015) 166–173.

[44] H. Liu, H. Fan, X. Gao, X. Huang, X. Liu, L. Liu, C. Zhou, J. Tang, Q. Wang, W. Liu, Design, synthesis and preliminary structure–activity relationship investigation of nitrogen-containing chalcone derivatives as acetylcholinesterase and butyrylcholinesterase inhibitors: a further study based on Flavokawain B Mannich base derivatives, *J. Enzyme Inhib. Med. Chem.* 31 (2016) 580–589.

[45] V. Thiagarajan, S.H. Lin, Y.C. Chang, C.F. Weng, Identification of novel FAK and S6K1 dual inhibitors from natural compounds via ADMET screening and molecular docking, *Biomed. Pharmacother.* 80 (2016) 52–62.

[46] Y. Nicolet, O. Lockridge, P. Masson, J.C. Fontecilla-Camps, F. Nachon, Crystal structure of human butyrylcholinesterase and of its complexes with substrate and products, *J. Biol. Chem.* 278 (2003) 41141–41147.

[47] B. Brus, U. Kosak, S. Turk, A. Pisljar, N. Coquelle, J. Kos, J. Stojan, J.P. Colletier, S. Gobec, Discovery, biological evaluation, and crystal structure of a novel nanomolar selective butyrylcholinesterase inhibitor, *J. Med. Chem.* 57 (2014) 8167–18179.

Figure Captions

Table 1

The chemical structures of compounds **3a–3x** and their inhibitory activities against EeAChE and eqBuChE. ^a

Table 2

LogP values of some compounds.

Table 3

ADME properties of active compounds.

Table 4

-CDOCKER_INTERACTION_ENERGY of title compounds **3a–3o** and 1POI.

Fig. 1. The rational design in this study.

Fig. 2. Lineweaver–Burk plots of eqBuChE inhibition kinetics of compounds **3f** (A) and **3o** (B). The Lineweaver–Burk secondary plots of compounds **3f** (C) and **3o** (D). Reciprocals of enzyme activity (eqBuChE) vs reciprocals of substrate (butyrylthiocholine iodide) with different concentrations (0–20 μM) of inhibitor. Inset: Concentrations used for inhibitor are coded with different graphic symbols.

Fig. 3. Cytotoxicity of compound **3o** and donepezil tested at concentrations in the range 1–50 μM in PC12 neurons for 24 h. Untreated cells were used as control. Results are expressed as percentage of cell survival vs untreated cell (control) and shown as mean \pm SD (n = 3).

Fig. 4. Neuroprotective effect on PC12 neurons of compound **3o**. After 24 h incubation at different concentration (10, 25 and 50 μM) with H_2O_2 (300 μM). Untreated cells were

used as control. Results represent mean \pm SEM ($n = 3$). Statistical significance was calculated using one-way ANOVA and Bonferroni post hoc tests. $^{###}p < 0.001$ compared with the control group; $^*p < 0.05$ compared with H₂O₂ group.

Fig. 5. The regression is based on ADMET_PSA_2D and ADMET_AlogP98, and the compounds set lie entirely within the 95% confidence ellipse. (Red and green ellipses describe 95 and 99% of HIA, respectively; pink and sky blue ellipses describe 95 and 99% of BBB, respectively).

Fig. 6. *Left:* 3D mode of interaction of compound **3o** and receptor BuChE (PDB code: 1P0I) analyzed by Discovery Studio 2017R2. Conventional Hydrogen Bond and Carbon Hydrogen bond and Alkyl as well as Pi-Alkyl are shown by green, light green and pink, respectively. *Right:* Two dimensional mode of interaction of compound **3o** and receptor BuChE (PDB code: 1P0I) analyzed by Discovery Studio 2017R2.

Fig. 7. The H-Bonds surface of compound **3o** and receptor BuChE (PDB code: 1P0I) analyzed by Discovery Studio 2017R2.

Scheme 1. Synthesis of compound **3**.

Reagents and conditions: (i) 40% NaOH/H₂O, acetone, 60°C; (ii) N₂H₄·H₂O, EtOH, reflux; (iii) R₂CHBrCOCl, DMAP, CH₂Cl₂; (iv) NaHCO₃, EtOH, 30–70°C.

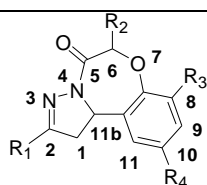
Scheme 2. Synthesis of two enantiomers of compound **3o**.

Reagents and conditions: (v) EDC·HCl, HOBT, CH₂Cl₂; (vi) NaHCO₃, EtOH, 60–70°C.

Table 1

The chemical structures of compounds **3a–3x** and their inhibitory activities against EeAChE and eqBuChE. ^a

Compound	R ₁	R ₂	R ₃	R ₄	IC ₅₀ , μM (or inhibition % at 20μM)	
					AChE ^b	BuChE ^c
3a	CH ₃	H	Cl	Cl	25±7%	31±8%
3b	CH ₃	CH ₃	Cl	Cl	22±7%	5.95±3.36
3c	CH ₃	Et	Cl	Cl	26±4%	4.67±2.40
3d	CH ₃	H	Br	Br	<i>d</i>	24±4%
3e	CH ₃	CH ₃	Br	Br	<i>d</i>	11±1%
3f	CH ₃	Et	Br	Br	41±7%	2.92±0.56
3g	CH ₃	H	H	Cl	2±2%	<i>d</i>
3h	CH ₃	CH ₃	H	Cl	<i>d</i>	39±1%
3i	CH ₃	Et	H	Cl	<i>d</i>	12.83±0.95
3j	CH ₃	H	H	Br	29±4%	<i>d</i>
3k	CH ₃	CH ₃	H	Br	23±3%	18±4%
3l	CH ₃	Et	H	Br	nt	39±6%
3m	CH ₃	H	Br	Cl	32±4%	18±4%
3n	CH ₃	CH ₃	Br	Cl	<i>d</i>	11.10±0.87
3o	CH ₃	Et	Br	Cl	<i>d</i>	2.04±0.74
(6R)-3o					<i>d</i>	1.14±0.40
(6S)-3o					<i>d</i>	20.42±5.30
3p	CH ₃	H	OCH ₃	H	34±2%	2±1%
3q	CH ₃	CH ₃	OCH ₃	H	24±2%	<i>d</i>
3r	CH ₃	H	H	CH ₃	24±4%	<i>d</i>
3s	CH ₃	CH ₃	H	CH ₃	22±3%	1±1%



3t	Fu	H	H	Br	25±5%	20±2%
3u	Fu	CH ₃	Cl	Cl	28±3%	23±3%
3v	4-F-Ph	H	Br	Br	<i>d</i>	<i>d</i>
3w	4-F-Ph	H	H	Br	<i>d</i>	45±5%
3x	4-F-Ph	H	H	Cl	<i>d</i>	17±1%
donepezil					0.028±0.010	11.81±0.60

^a Each IC₅₀ value is the mean ± SEM from three experiments (*n* = 3).

^b AChE from electric eel.

^c BuChE from horse serum.

^d No inhibitory activity (%) against either EeAChE or eqBuChE at 20 μM.

Table 2

LogP values of active compounds.

Compound	logP ^a
3b	2.49
3c	1.12
3f	1.08
3i	1.05
3l	1.11
3n	2.18
3o	1.57

^a Octanol–water partition coefficients of some compounds were measured by the shake flask method with slight modification.

Table 3

ADME properties of active compounds.

Compound	A ^a	D ^b	M ^c	E ^d	ALogP98 ^e	PSA2D ^f	
3b	0	2	2	0	2	2.560	40.906
3c	0	2	1	0	2	3.084	40.906
3f	0	2	1	0	1	3.252	40.906
3i	0	3	2	0	2	2.419	40.906

3l	0	2	2	0	1	2.503	40.906
3n	0	2	1	0	1	2.644	40.906
3o	0	2	1	0	2	3.168	40.906

^a Absorption: Intestinal absorption.

^b Distribution: Aqueous solubility and Blood-brain barrier penetration.

^c Metabolism: CYP2D6.

^d Excretion: Plasma protein binding.

^e ALogP98: Predicted octanol/water.

^f PSA: polar surface area, 2D: two-dimensional.

Table 4

-CDOCKER_INTERACTION_ENERGY of title compounds **3a–3o** and 1POI.

Compd.	-CDOCKER_INTERACTION_ENERGY ΔG (kcal/mol)
3a	34.3266
3b	37.5403
3c	39.4205
3d	34.1125
3e	35.3028
3f	36.3670
3g	31.0356
3h	33.5276
3i	35.5948
3m	33.7530
3n	36.0392
6R-3o	40.1013
6S-3o	35.4629

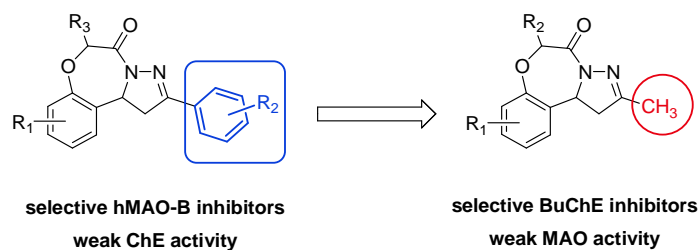


Fig. 1. The rational design in this study.

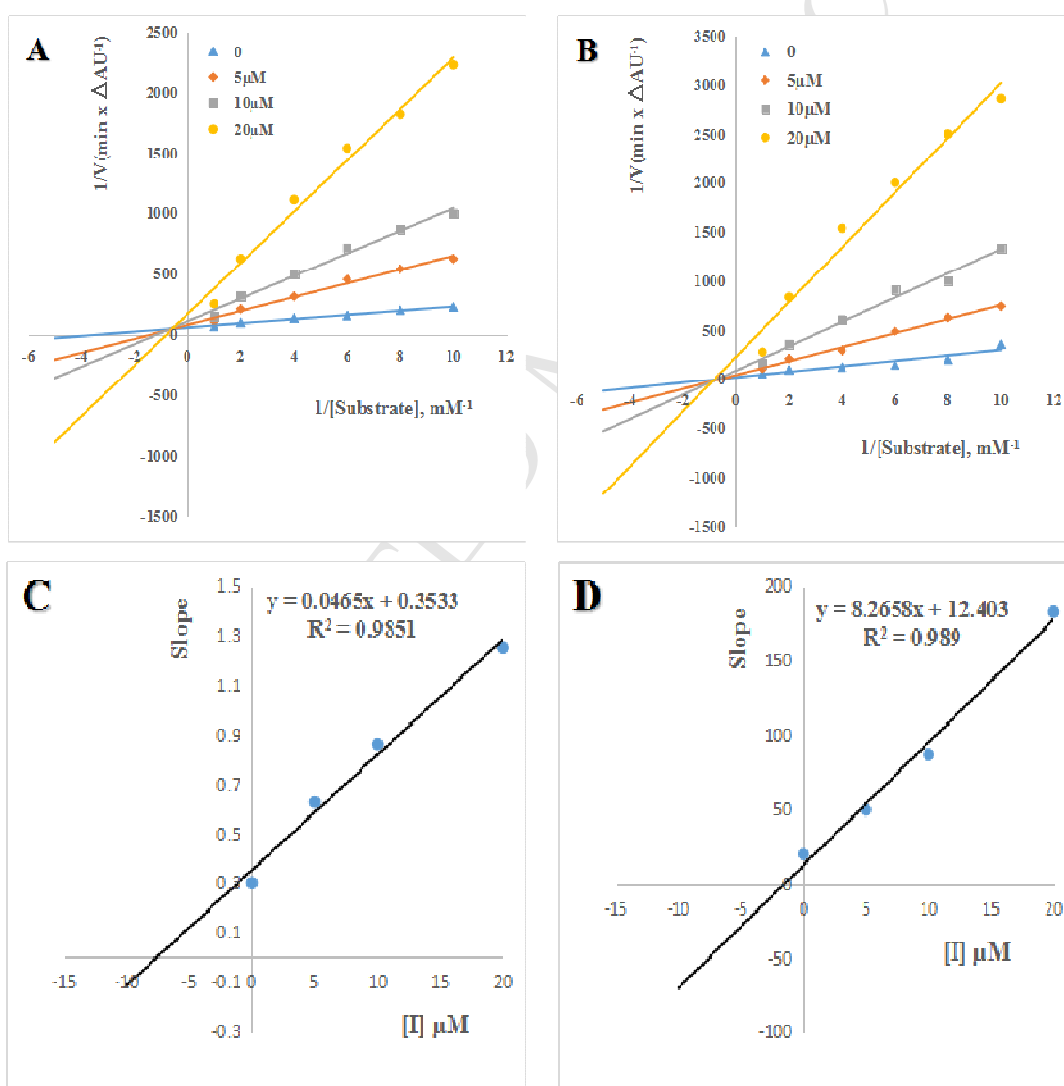


Fig. 2. Lineweaver–Burk plots of eqBuChE inhibition kinetics of compounds **3f** (A) and **3o** (B). The Lineweaver–Burk secondary plots of compounds **3f** (C) and **3o** (D).

Reciprocals of enzyme activity (eqBuChE) vs reciprocals of substrate (butyrylthiocholine iodide) with different concentrations (0–20 μM) of inhibitor. Inset: Concentrations used for inhibitor are coded with different graphic symbols.

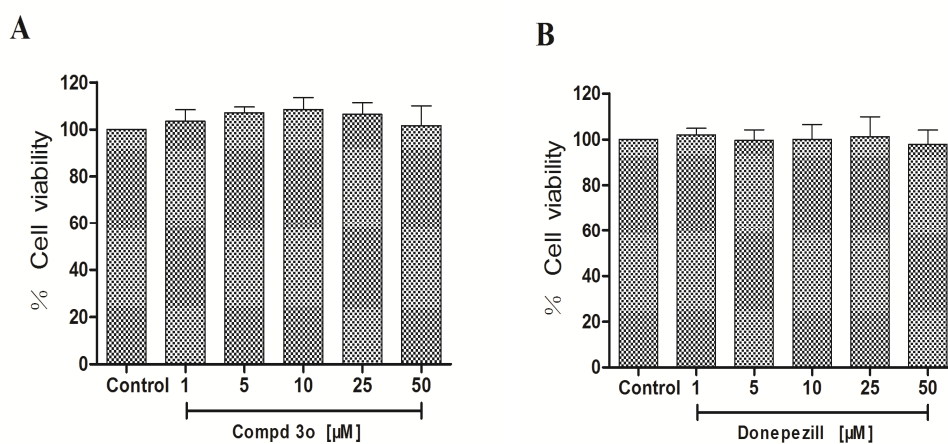


Fig. 3. Cytotoxicity of compound **3o** and donepezil tested at concentrations in the range 1–50 μM in PC12 neurons for 24 h. Untreated cells were used as control. Results are expressed as percentage of cell survival vs untreated cell (control) and shown as mean \pm SD (n = 3)

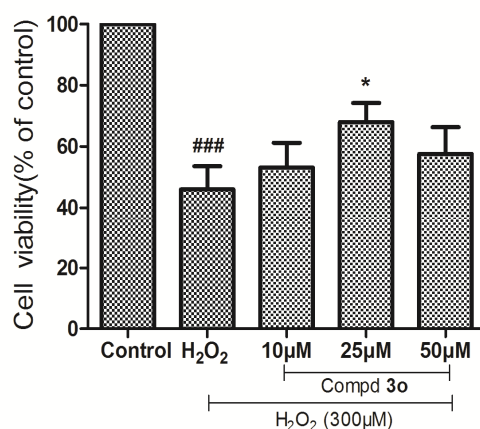


Fig. 4. Neuroprotective effect on PC12 neurons of compound **3o**. After 24 h incubation at different concentration (10, 25 and 50 μM) with H_2O_2 (300 μM). Untreated cells were used as control. Results represent mean \pm SEM (n = 3). Statistical significance was

calculated using one-way ANOVA and Bonferroni post hoc tests. $###p < 0.001$ compared with the control group; $*p < 0.05$ compared with H₂O₂ group.

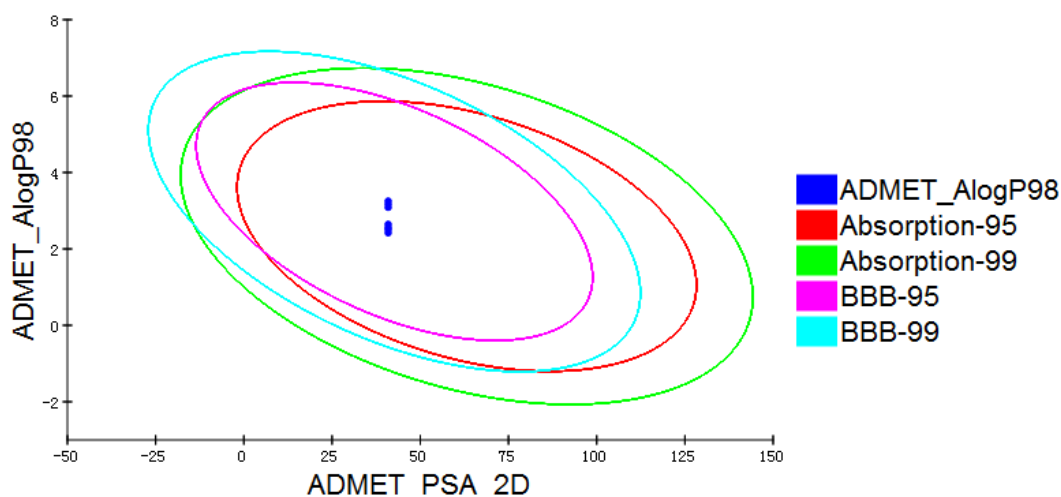


Fig. 5. The regression is based on ADMET_PSA_2D and ADMET_AlogP98, and the compounds set lie entirely within the 95% confidence ellipse. (Red and green ellipses describe 95 and 99% of HIA, respectively; pink and sky blue ellipses describe 95 and 99% of BBB, respectively).

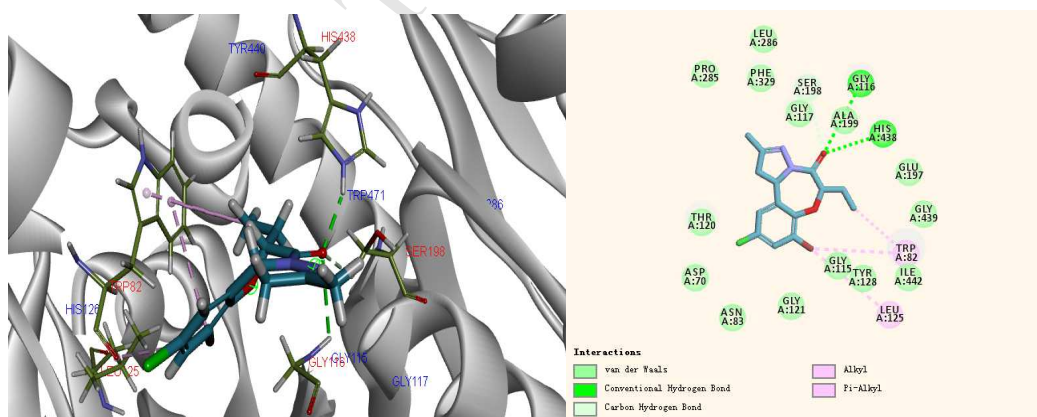


Fig. 6. Left: 3D mode of interaction of compound **30** and receptor BuChE (PDB code: 1P0I) analyzed by Discovery Studio 2017R2. Conventional Hydrogen Bond and Carbon Hydrogen bond and Alkyl as well as Pi-Alkyl are shown by green, light green and pink,

respectively. *Right:* Two dimensional mode of interaction of compound **30** and receptor BuChE (PDB code: 1P0I) analyzed by Discovery Studio 2017R2.

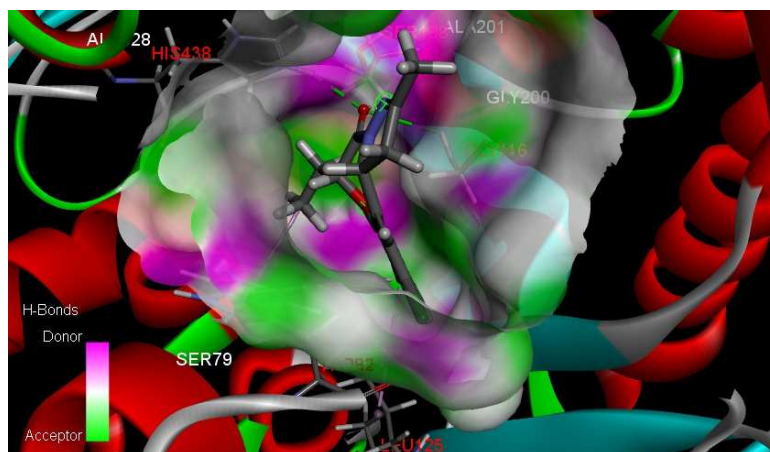
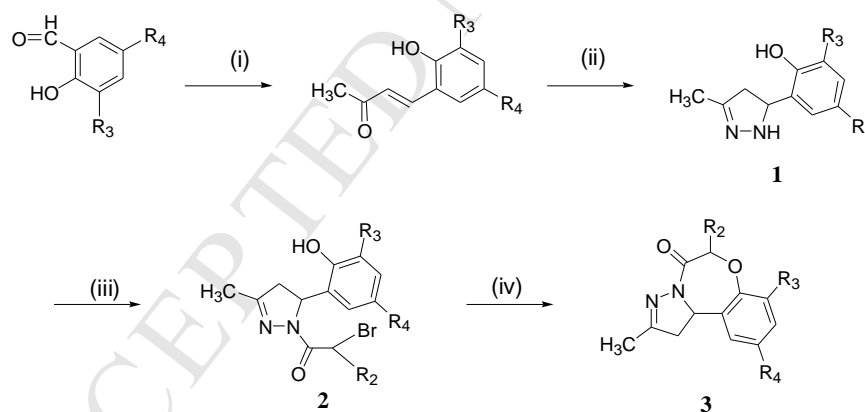
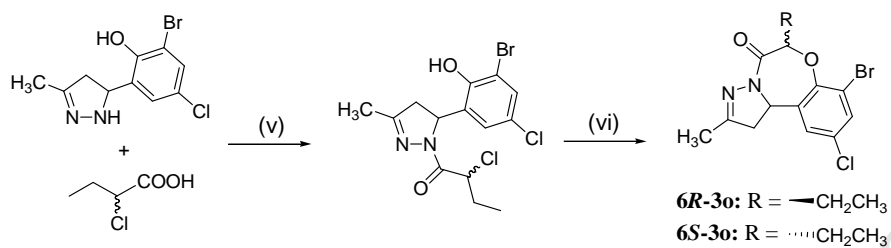


Fig. 7. The H-Bonds surface of compound **30** and receptor BuChE (PDB code: 1P0I) analyzed by Discovery Studio 2017R2.



Scheme 1. Synthesis of compound **3**.

Reagents and conditions: (i) 40% NaOH/H₂O, acetone, 60°C; (ii) N₂H₄·H₂O, EtOH, reflux; (iii) R₂CHBrCOCl, DMAP, CH₂Cl₂; (iv) NaHCO₃, EtOH, 30–70°C.



Scheme 2. Synthesis of two enantiomers of compound **30**.

Reagents and conditions: (v) EDC·HCl, HOBT, CH₂Cl₂; (vi) NaHCO₃, EtOH, 60–70°C.

Highlights

- Tricyclic compounds are reversible, selective BuChE inhibitors.
- Dihalogen and 6-ethyl substituent improve BuChE activity.
- IC₅₀ values of **3f** and **3o** are 2.95 and 2.04 μ M, respectively.
- Compound **3o** exhibited remarkable neuroprotective activity.